ISBN: 978-3-95450-247-9 ISSN: 2673-5490 doi: 10.18429/JACoW-IPAC2024-THPC73

COMBINED WAKEFIELD AND BEAM-BEAM EFFECTS IN THE EIC DESIGN*

J. Qiang†, LBNL, Berkeley, USA
M. Blaskiewicz, BNL, Upton, USA

Abstract

Collective wakefield and beam-beam effects play an important role in accelerator design and operation. These effects can cause beam instability, emittance growth, and luminosity degradation, and warrant careful study during accelerator design. In this paper, we report on the development of a computational capability that combines both short and long range wakefield models and a strong-strong beam-beam simulation model. Applications to the EIC will be discussed.

INTRODUCTION

The electron-ion collider (EIC) as the next generation collider for high energy nuclear physics research is being actively studied [1]. The EIC consists of two colliding rings, a hadron ring of 41-275 GeV and an electron storage ring of 5-18 GeV. The nominal design goal is to attain a peak luminosity of $10^{34}\mathrm{cm}^{-2}\mathrm{s}^{-1}$. Such a luminosity requires high electron and proton beam currents. The coherent instability driven by impedance becomes a major concern. Such an instability depends on the choice of transverse tune working points as well as beam bunch intensities. On the other hand, the nonlinear beam-beam interaction of two colliding beams produces tune spread in each beam. This tune spread provides Landau damping to the coherent instability and mitigate the instability in some regime [2, 3]. In other regimes, the coherent instability is still observed even with the presence of the beam-beam interaction.

COMPUTATIONAL MODEL

Wakefield Simulation Model

Wakes are simulated using standard binning techniques and fast Fourier transforms [4]. Transverse multibunch effects are handled assuming coupled bunch mode s while tracking one bunch. On turn n one generates the dipole moment of the tracked bunch at a fixed azimuth (say 0),

$$D_x^0(t,n) = I(t) < x(t) >$$

where $I(t)$ is the instantaneous bunch current and $< x(t) >$ is the centroid of the bunch as it passes. The moment associated with the angular offset is,

$$D_p^0(t,n) = I(t)[\beta_x < x'(t) > +\alpha_x < x(t) >].$$

Assuming the coherent tune shift is small, define the dipole moment for all subsequent bunches passing this location on turn n,

$$D_x(t,n) = \sum_{m=0}^{M-1} D_x^0(t - mT_b, n)\cos(m[\psi_\beta - \psi_s])$$
$$+D_p^0(t - mT_b, n)\sin(m[\psi_\beta - \psi_s]). \quad (1)$$

Where there are M bunches with period T_b. The betatron phase advance between bunches is $\psi_\beta = 2\pi Q_x/M$ and the coupled bunch phase shift between bunches is $\psi_s = 2\pi s/M$. The long range wakes are modeled as a sum of damped oscillators and efficient expressions can be obtained to evaluate the wakes driven by (1).

The wakefield model of the EIC proper has been steadily improving since 2019 [5]. Wakes for individual components of the Electron Storage Ring have been modeled using CST, GdfidL and ECHO. The vertical long range wake is dominated by the resistive wall and the horizontal one is dominated by the fundamental mode of the crab cavities. The Hadron Storage Ring broadband impedance can be well characterized by a broadband resonator. The horizontal long range wake is dominated by the fundamental mode of the crab cavities and direct RF feedback has been modeled to reduce the apparent impedance.

Strong-Strong Beam-Beam Simulation Model

The beam-beam interaction is simulated using a strong-strong beam-beam code, BeamBeam3D [6, 7]. The BeamBeam3D is a parallel three-dimensional particle-in-cell code to model beam-beam effects in high-energy ring colliders. This code includes a self-consistent calculation of the electromagnetic forces (beam-beam forces) from two colliding beams (i.e. strong-strong modeling), a linear and nonlinear high-order transfer map model for beam transport between collision points, a stochastic map to treat radiation damping, quantum excitation, a single map to account for chromaticity effects, a feedback model, an impedance model, and a Bremsstrahlung model. Here, the beam-beam forces can be from head-on collision, offset collision, and crossing angle collision. These forces are calculated by solving the Poisson equation using a shifted integrated Green function method, which can be computed very efficiently using an FFT-based algorithm on a uniform grid. For the crossing angle collision, two colliding beams are transformed from the lab frame into a boosted Lorentz frame [8, 9], where the beam-beam forces are calculated in the same way as the head-on collision. After the collision the particles are transformed back into the laboratory frame. The BeamBeam3D code can also handle multiple bunches from each beam collision at multiple interaction points (IPs) and include models for conducting wire and crab cavity compensations.

* Work supported by the U.S. DOE under Contract No. DE-AC02-05CH11231.
† jqiang@lbl.gov

ISBN: 978-3-95450-247-9 ISSN: 2673-5490 doi: 10.18429/JACoW-IPAC2024-THPC73

INTERPLAY BETWEEN BEAM-BEAM AND WAKEFIELD EFFECTS

The parameters used in this study is from Table 4.15 of the EIC CDR design report [1]. Here, a 275 GeV proton beam collides with a 10 GeV electron beam with a 25 mrad collision angle. The proton beam has a single bunch population of 0.688×10^{11}, and electron beam 1.72×10^{11}. The beam-beam parameters for the proton beam are $(0.012, 0.012)$ and $(0.072, 0.1)$ for the electron beam. The nominal transverse working point tunes are $(29.228, 30.210)$ for the proton beam, and $(51.08, 48.06)$ for the electron beam. In this study, we first check how the electron beam and the proton beam behave with only the wakefield effects. Figure 1 shows the electron beam logarithm of average vertical action and proton beam average horizontal action evolution without the beam-beam effects. It is seen that electron beam vertical average action becomes unstable and grows exponentially after 1000 turns. This instability is caused by the long-range vertical resistive wall wakefield. The proton beam horizontal average action shows unstable growth. This instability is due to the long-range wakefield of crab cavities in the EIC.

Next, we turn on the beam-beam interaction in the EIC using the strong-strong model in the BeamBeam3D. Figure 2 shows the electron beam logarithm of average vertical action and proton beam average horizontal action evolution with both the wakefield and the beam-beam effects. Both electron beam and proton beam become stable in the horizontal and vertical dimensions. This is due to the fact that the nonlinear beam-beam interaction induces a tune spread. This tune spread provides a Landau damping for the instability and suppresses the instability.

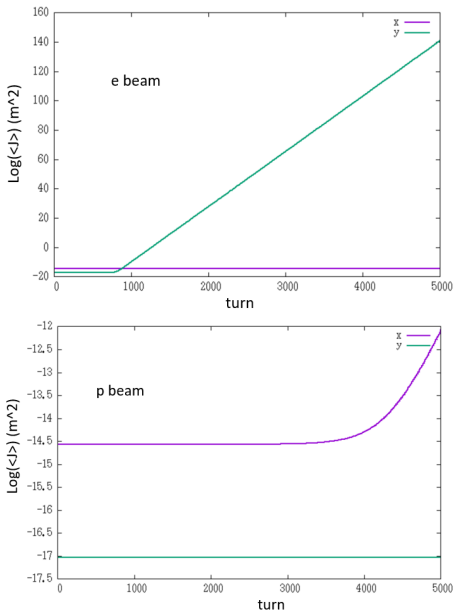

Figure 1: Electron beam logarithm average action (top) and proton beam logarithm average action (bottom) evolution without beam-beam effects.

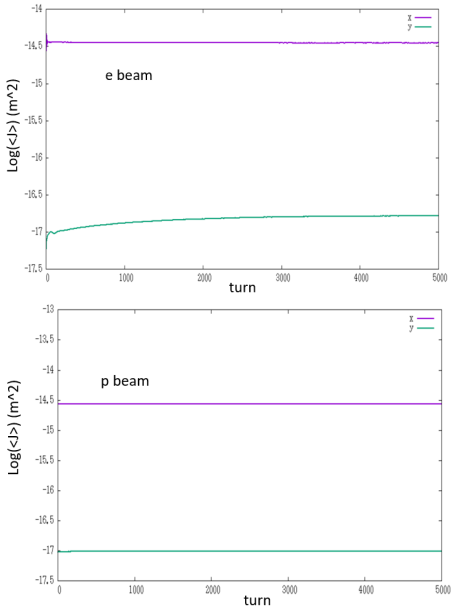

Figure 2: Electron beam logarithm average action (top) and proton beam logarithm average action (bottom) evolution with both wakefield and beam-beam effects.

EFFECTS OF CRAB CAVITY VOLTAGE ON BEAM INSTABILITY

In order to compensate the geometric luminosity loss from crossing angle collision, in the EIC, two group of crab cavities located at 90 degree phase advance away from the interaction point (IP) on both sides of the IP are used to correct the collision angle so that two beams collide head-on at the IP. The voltage of the crab cavity is set as [10]:

$$V_{nominal} = \frac{Ec\tan(\theta_c/2)}{q\omega\sqrt{\beta^*\beta_{cc}}} \quad (2)$$

This nominal voltage will fully compensate crossing angle at the IP. In practical operation, if there is a RF power loss or other accident, the crab cavity might not be able to operate with the nominal voltage. Figure 3 shows the electron beam average vertical action and the proton beam average horizontal action evolution with several crab cavity voltages. Without RF power inside the crab cavity, strong instability is seen in both electron beam and the proton beam. Even with 0.6× nominal voltage, both beams still become unstable until 0.7× nominal voltage is restored inside the cavity. Losing voltage inside the crab cavity results in less correction of crossing angle and weaker beam-beam interaction. This causes the shrink of tune spread and the loss of Landau damping to the instability.

IMPEDANCE BUDGET WITH BEAM-BEAM EFFECTS

The wakefields used in this study are based on the nominal EIC design. It would be interesting to know how far one can deviate from these designed values. The long-range

ISBN: 978-3-95450-247-9 ISSN: 2673-5490 doi: 10.18429/JACoW-IPAC2024-THPC73

crab cavity wakefield is the dominant factor causing proton beam instability. This wakefield is characterized by a frequency, a damping rate, and an amplitude. Figure 4 shows the electron beam vertical average action and proton beam horizon average action evolution with the nominal damping rate, 0.85× the nominal damping rate, and 0.75× damping rate. A 25% reduction in damping rate causes the proton beam to become unstable. There is not a lot of margin of the damping rate in the crab cavity design with only direct RF feedback.

The long-range vertical resistive wall wakefield contributes to the electron beam instability. Figure 5 shows the electron beam vertical average action and proton beam horizon average action evolution with 4× the nominal wakefield amplitude, 4.1×, and 4.2× the nominal amplitude. The electron becomes unstable with 4.2× nominal amplitude. This gives a large margin in the electron ring for such an instability.

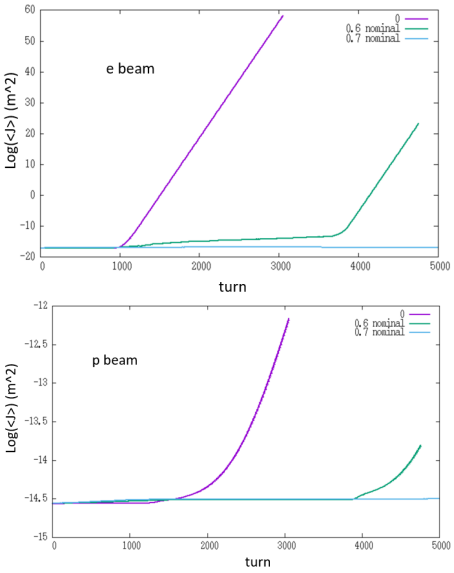

Figure 3: Electron beam logarithm vertical average action (top) and proton beam logarithm horizontal average action (bottom) evolution with 0×, 0.6×, and 0.7× nominal voltages.

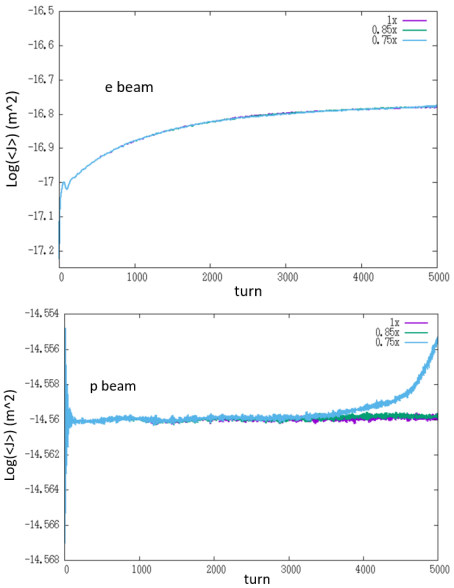

Figure 4: Electron beam logarithm vertical average action (top) and proton beam logarithm horizontal average action (bottom) evolution with 1×, 0.8×, and 0.75× nominal damping rate.

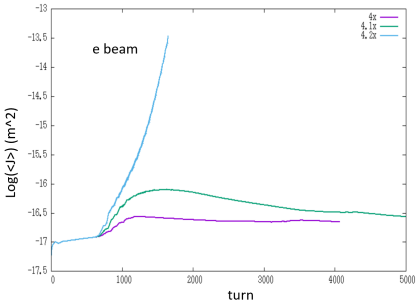

Figure 5: Electron beam logarithm vertical average action evolution with 4×, 4.1×, and 4.2× nominal electron ring resistive wall wakefield amplitude.

PROTON BEAM TUNES ON BEAM INSTABILITY

The instability of colliding beams depends on the tunes of each beam. In this study, we fixed the working tunes of the electron beam, and scanned the working tunes of the proton beam. Figure 6 shows the logarithm of the final normalized electron vertical average action and proton horizontal average action as a function of proton beam horizontal and vertical tune. Two strong instability stopbands are seen in this plot. One is around proton beam horizontal 0.15, the other one is around 0.375. At the 0.15 horizontal tune, strong coherent beam-beam oscillation is observed. This oscillation causes the coherent mode outside the incoherent tune spread that provides the Landau damping to the instability. The second strong stopband around 0.375 might be caused by the interaction between wakefields and high order beam-beam resonance. This stopband is not seen in the weak-strong or soft-Gaussian beam-beam interaction model.

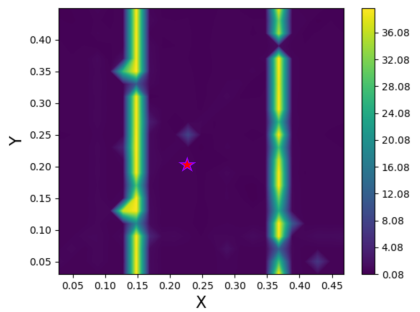

Figure 6: Final electron beam logarithm normalized vertical average action versus proton beam transverse tunes.

ISBN: 978-3-95450-247-9 ISSN: 2673-5490 doi: 10.18429/JACoW-IPAC2024-THPC73

REFERENCES

[1] J. Beebe-Wang ed., "Electron-Ion-Collider at Brookhaven National Laboratory Conceptual Design Report,", 2021, https://www.bnl.gov/EC/files/EIC_CDR_Final.pdf.

[2] M. G. Minty *et.al.*, "Recent beam-beam experience with multiple high current bunches in PEP-II", SLAC-PUB-8202, 2000. doi:10.2172/753279

[3] R. Li and M. Blaskiewicz, "Impact of choherent beam-beam interaction on the landau dampling of the transverse coupled-bunch instability", in *Proc. IPAC'21*, Campinas, SP, Brasil, pp. 2062–2065. doi:10.18429/JACoW-IPAC2021-TUPAB258

[4] M. Blaskiewicz, "The TRANFT User's Manual", BNL-77074-2006-IR, 2006.

[5] A. Blednykh *et.al.* "An Overview of the Collective Effects and Impedance Calculation for the EIC", in *Proc. IPAC'21*, Campinas, SP, Brasil, pp. 4266–4269. doi:10.18429/JACoW-IPAC2021-THPAB238

[6] J. Qiang, M. A. Furman, and R. D. Ryne, "Strong-strong beam-beam simulation using a Green function approach," *Phys. Rev. Spec. Top. Accel. Beams*, vol. 5, no. 10, Oct. 2002. doi:10.1103/physrevstab.5.104402

[7] J. Qiang, M. A. Furman, and R. D. Ryne, "A parallel particle-in-cell model for beam-beam interaction in high energy ring colliders," *J. Comput. Phys.*, vol. 198, no. 1, pp. 278-294, Jul. 2004. doi:10.1016/j.jcp.2004.01.008

[8] K. Hirata, "Analysis of beam-beam interactions with a large crossing angle, " *Phys. Rev. Lett.*, vol. 74, no. 12, p. 2228, 1995. doi:10.1103/PhysRevLett.74.2228

[9] L. H. A. Leunissen, F. Schmidt, and G. Ripken, "Six-dimensional beam-beam kick including coupled motion," *Phys. Rev. Spec. Top. Accel. Beams*, vol. 3, p. 124002, 2000. doi:10.1103/PhysRevSTAB.3.124002

[10] J. Qiang *et al.*, "Simulation of beam–beam interaction with crab cavities for LHC upgrade," *Nucl. Instrum. Methods Phys. Res., Sect. A*, vol. 900, pp. 53-59, 2018. doi:10.1016/j.nima.2018.05.055